



Vancouver, Canada

May 31 – June 3, 2017/ *Mai 31 – Juin 3, 2017*

## **AN INVESTIGATION OF THE DISTRIBUTION OF MOBILE CRANE LOADS FOR CONSTRUCTION PROJECTS**

Lin, Meng<sup>1</sup>, Duong, Nguyet (Lisa)<sup>2</sup>, Deng, Lijun<sup>3</sup>, Hermann, Ulrich (Rick)<sup>4</sup>, Zubick, Travis<sup>5</sup>, Lei, Zhen<sup>6</sup>, and Adeeb, Samer<sup>7,8</sup>

<sup>1, 2, 3, 7</sup> University of Alberta, Canada

<sup>4, 5, 6</sup> PCL Industrial Management Inc., Canada

<sup>8</sup> [adeeb@ualberta.ca](mailto:adeeb@ualberta.ca)

**Abstract:** In the Canadian construction industry, mobile cranes, such as rough terrain cranes and crawler cranes are employed to perform lifting for construction projects. Over the years, the ground preparation below load-spreading mats supporting the mobile crane has been mainly designed based on crude assumptions or using rules of thumb, due to the lack of reference data regarding the actual loads transferred to the ground. This paper aims to obtain the actual reactions beneath the outrigger supports for a rough terrain crane based on the collections of adequate numbers of experimental data. The load data were recorded from the earth pressure cells buried vertically in the ground at two different depths at three critical boom positions with three working radii during the lifting operations. The experimental data were compared with others obtained from currently common used methods, such as the 2:1 approximation method, Boussinesq equations and the software predictions provided by crane manufacture. In addition, the soil-mat interaction was simulated with a two-dimensional (2D) axisymmetric model using the finite element analysis (FEA). This study indicates that the prediction of ground bearing pressure (GBP) beneath outrigger supports from the crane software is reliable but should be increased by 10%.

### **1 Introduction**

In the Canadian construction industry, mobile cranes, such as rough terrain and all-terrain cranes are employed to perform lifts in industrial and infrastructure projects. The mobile crane support systems need to be carefully designed to ensure the factor of safety (FS) against potential instabilities, such as the crane tip-over. In practice, the crane manufacturer reduces the crane capacities to a percentage of the load that can either tip the crane over or cause structural damage. According to both ASMEB30.5 and CSA Z150, this percentage shall not exceed 85% for wheel-mounted cranes with outriggers fully extended and set (FS = 1.176). However, the subgrade ground bearing pressure factor of safety of 2 is usually employed for mobile cranes in construction industry, such as PCL Industrial Management Inc.

A number of research projects addressed the immediate and consolidation settlement of shallow foundations (Duncan and Buchignani, 1987; Lee and Salgado, 2002; Salgado, 2008). The crane mats can be treated as shallow foundations in this context. Although the theory of foundation settlement has been studied in the past, there is a lack of research that tackles the measurement of in-situ soil stress under flexible mats and a combined load pattern. In practice, the long term settlement is not an issue for cranes, because cranes have relatively shorter loading durations than buildings. It is expected that the settlement will be immediate due to the elasto-plastic response of the soils to the mat pressure. However, previous studies and field observations have shown that these short term settlements are not a major problem because they can be very small for properly prepared crane mats. Therefore, the focus of crane mat design is the bearing capacity of soils. Although there has been extensive research for the bearing capacity of soils

for shallow foundations (Terzaghi, 1943; Meyerhof, 1956; Vesic, 1973), there is lack of a specific method for the calculation of bearing capacity of soils underneath cranes. A factor of safety between 1.5 and 2.0 was suggested by Shapiro et al. (1999) and research institute, CIRIA (1996) in calculating the allowable bearing capacity for cranes supported by outriggers. In the absence of accurate value of allowable soil bearing capacity for mobile cranes, Shapiro & Shapiro (2011) provided presumptive soil bearing capacity for various soils. In addition, PCL Industrial Management Inc., usually prepares the ground for an allowable GBP between 167 kPa (3500 psf) and 239 kPa (5000 psf) during lifting operations by adding compacted gravel layers and adds timber mats to help distribute the crane loads. For module assembly facilities heavy laydown areas, 287 kPa (6000 psf) is usually specified.

Due to the lack of reference data regarding the actual loads transferred to the ground, the ground preparations and crane support systems have been designed based on crude assumptions or using rules of thumb. Shapiro & Shapiro (2011) summarized the currently used theoretical method in calculating the crane loads on the supporting ground. For a rough terrain crane, the method assumes the crane carrier and outriggers to be inelastic and ground support to be linear elastic, and applies the rigid body theory for distributing outrigger loads. For a crawler crane, the method assumes the crawler frames and carbody to be absolutely rigid, and the pressure diagram under the crawler tracks is either triangular or trapezoidal. Crawler cranes will be analyzed in a future paper, but the methodology of using pressure sensors in this research is being validated before more expensive field testing. Based on these assumptions, crane manufacturers routinely supply software to calculate the crane outriggers forces or crawler track pressures imposed by a specific crane with a specific configuration, such as Tadano's Outrigger Reaction Force Supply Service (<https://www.tadano.co.jp/service/data/tdnsys/jackale/register.asp>) and Liebherr's LICCON computer system (<https://www.liebherr.com/en/sau/products/mobile-and-crawler-cranes/mobile-cranes/mobile-crane-technology/crane-controller/crane-controller.html>).

The safe design of the supporting systems relies on the accuracy of estimating the reactions under the crane outriggers or crawler tracks, and ensures that the developed pressure underneath the supporting structure are lower than the allowable ground bearing pressure. This paper aims to obtain the actual reactions beneath the outrigger supports for a rough terrain crane based on the collections of adequate numbers of experimental data. The pressure data was recorded from the earth pressure cells buried in crucial locations beneath the ground at various stages during the lifting operations, when the boom swings from the front, to the corner, and to the side of the crane. In addition, the experimental results were compared with others obtained from currently common used methods, such as the 2:1 approximation method, the Boussinesq equations, the software calculations provided by crane manufactures, and the finite element analysis (FEA) using Abaqus.

## **2 Investigation of reactions under outrigger supports**

In November 2015, 3 sets of lifting experiments were performed on a rough terrain crane at PCL East module yard located in Edmonton, Alberta. The Tadano GR-600XL was selected to lift and move the heavy loads from the front of the crane, to the corner, and to the side of the crane with three different working radii, and thus a total of 9 sets of data were collected (1 set for each radius and boom position). The ground bearing pressure (GBP) beneath one of the supporting pads was measured using 2 earth pressure cells, respectively buried 4" (0.1016 m) and 10" (0.254 m) below the ground surface. The measured GBP distribution along the depth was compared to the 2:1 approximation method, the Boussinesq equations, and the finite element analysis (FEA) using Abaqus.

### **2.1 Test Designs**

Tadano GR-600XL Rough Terrain Crane with a hook block capacity of 60 ton (Figure 3a) was selected to lift and move the load weights. Four outriggers were fully extended with the spread of 7.2 m and the four wheels were completely elevated above the ground. The telescoping boom was extended with a boom length of 18.83 m with the jib stowed in. Two concrete lock blocks with the total weight of 3765 kg (8300 lbs) were lifted together and moved as the boom swung. The total lifting weight including the load, crane block, auxiliary hook ball, sheave and rigging was measured to be 4808 kg (10600 lbs) on the crane scale during lifting operations. Three sets of tests with different working radii of 9.144 m (30'), 12.192 m (40'), and 15.24 m (50') were performed. Their corresponding boom angles, lifting heights, rated lifting capacities are all summarized in Table 1. The boom lifting the loads was slewed from the front of the crane ( $\alpha = 180^\circ$ ) to

the side of the crane ( $\alpha = 90^\circ$ ), passing over outrigger 1 ( $\alpha = 135^\circ$ ), and was stopped at these three locations to record the pressure readings from the two pressure cells buried under outrigger 1 (Figure 1).

The outrigger reaction force was calculated using the Tadano supplied program. The values were obtained when the boom passed over outrigger 1 ( $\alpha = 135^\circ$ ), and were 185 kN, 228 kN and 275 kN corresponding to three working radii. The total earth pressure cells were provided by RST Instruments Ltd. and used to measure the GBP at specific locations (<http://www.rstinstruments.com/Total-Earth-Pressure-Cell.html>). During the tests, the data was recorded every 10 seconds using the DT2055B data logger which is capable of monitoring up to 5 wired sensors (<http://www.rstinstruments.com/DT2055B-5-10-Channel-Vibrating-Wire-Thermistor-Data-Logger.html>). A small trench (width x length x depth = 2' x 4' x 1' = 0.6096 m x 1.2192 m x 0.3048 m) was dug in the ground in which the two pressure cells were buried. As shown in Figure 2, The trench was filled in with compact sand and the upper and lower pressure cells were respectively placed at 4" (0.1016 m) and 10" (0.254 m) below the ground (Figure 2). Total of 4.5"x42" diameter outrigger mats made of plywood were placed below the crane outriggers to reduce the GBP during the lifting operations. Each outrigger mat was composed by three layers of 3/4" plywood (Figure 3b). Existing module yard ground conditions were compacted gravel in good condition.

Table 1: Test information corresponding to three radii at  $\alpha = 135^\circ$

Location: PCL East Mod Yard in Edmonton, Alberta Date of Lift: 11/04/2015 Crane: Tadano GR-600XL with telescoping boom (18.8m) and fully extended outriggers	Test 1	Test 2	Test 3
Test radius (m)	9.144	12.192	15.240
Boom angle ( $^\circ$ )	56.8	44.3	27.2
Lifting height (m)	18.8	16.0	11.4
Chart capacity (kg)	17554	10705	6532
Measured total lifting weight (kg)	4808	4808	4808
Percent crane capacity (%)	27	45	74
Software calculated reaction force under outrigger 1(kN)	185	228	275
Plywood Outrigger mats Diameter (m)	1.0668	1.0668	1.0668
Calculated GBP beneath mat (kPa)	207	255	308

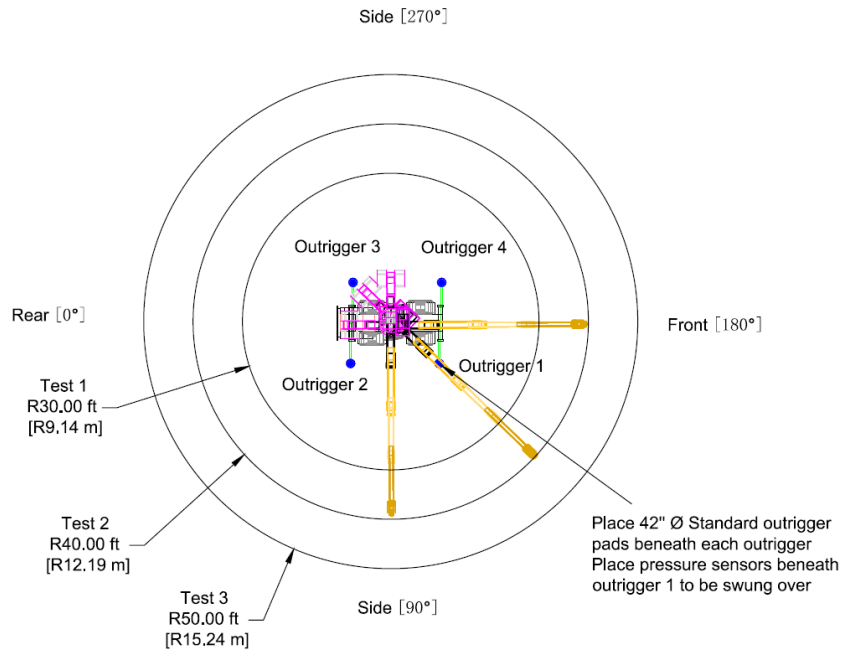


Figure 1: Lift plan for crane Tadano GR 600XL at PCI East Mod yard in Edmonton, Alberta

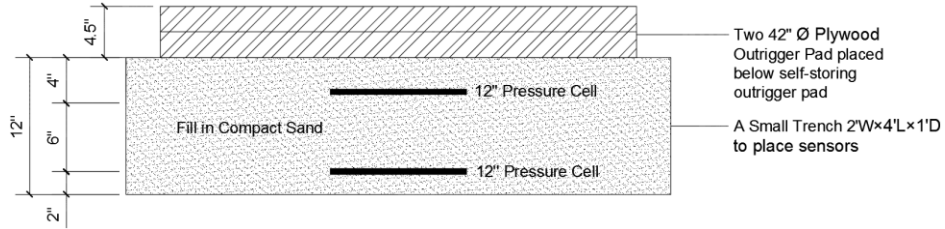


Figure 2: Pressure cells location buried in the ground

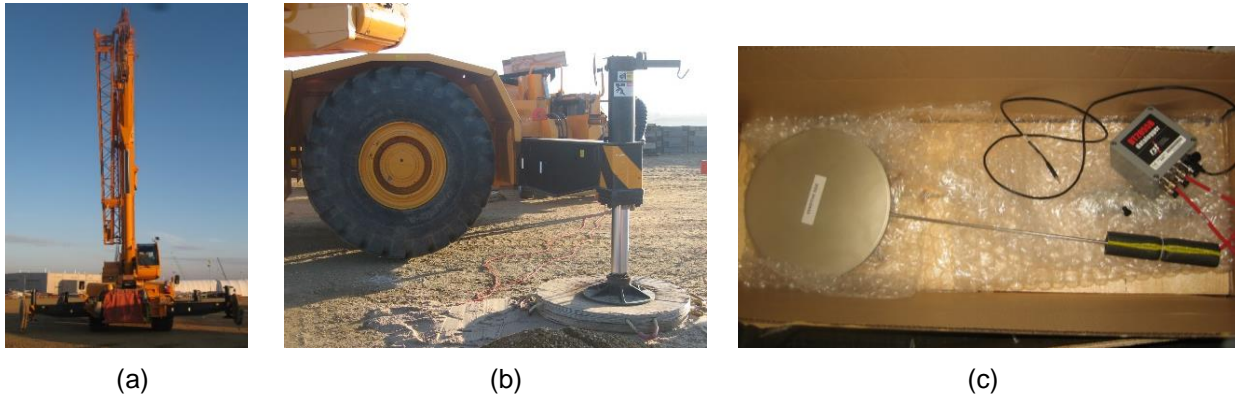


Figure 3: (a) test rough terrain crane, (b) plywood mats under the self-storing outrigger pad, and (c) LPTPC12-V total earth pressure cell and DT2055B data logger

## 2.2 Test Results

The test results corresponding to three test radii are summarized in Table 2. The highest GBP occurred when the boom passed over outrigger 1 with the largest working radius of 15.24 m. It is suggested to upgrade the ground conditions because the measured GBP of 271 kPa was close to the allowable GBP of 287 kPa (6000 psf) prepared for the test ground. The GBP measured at 4'' (0.1016 m) below the ground surface was about 3.2% lower than the values calculated at the ground surface, but the difference was relatively fluctuant with a standard deviation of 7.5%. The GBP measured at 10'' (0.254 m) below the ground surface was about 19.2% lower than the values measured at 4'' below the ground surface, and this reduction along the depth was relatively stable with a standard deviation of 0.5%. In comparison with the measured GBP in the three test working radii, the GBP at the same depth increases as the crane working radius increases because of the increase of the reaction force distributed to the outrigger. However, the reduction of GBP from 4'' to 10'' beneath the ground is consistent for the various crane working radii and the outrigger reaction force.

Table 2: Test results corresponding to three test radii at  $\alpha = 135^\circ$

Working radius	Software calculated reaction force at outrigger 1 (kN)	Boom location	GBP calculated at ground surface $\sigma_0$ (kPa)	GBP measured at 4'' below ground $\sigma_4$ (kPa)	GBP measured at 10'' below ground $\sigma_{10}$ (kPa)	Comparisons of GBP at different depth	
						$\frac{\sigma_4 - \sigma_0}{\sigma_0}$	$\frac{\sigma_{10} - \sigma_4}{\sigma_4}$
9.144 m (30')	185	Front	178	168	136	-5.6%	-19.0%
		Outrigger	207	191	154	-7.7%	-19.4%
		Side	178	181	146	1.7%	-19.3%
12.192 m (40')	228	Front	205	192	157	-6.3%	-18.2%
		Outrigger	255	227	184	-11.0%	-18.9%
		Side	205	214	172	4.4%	-19.6%
15.24 m (50')	275	Front	229	222	180	-3.1%	-18.9%
		Outrigger	308	271	219	-12.0%	-19.2%
		Side	232	257	205	10.8%	-20.2%
Average $\pm$ standard deviation						-3.2% $\pm$ 7.5%	-19.2% $\pm$ 0.5%

### 2.3 Comparisons between the experimental results and predictive models

The two most often used methods in predicting the GBP (vertical stress) caused by the reaction force transferred from the outrigger mats to the ground underneath are the 2:1 approximation method and the Boussinesq equations. Both methods are based on the theory of elasticity. The 2:1 approximation method assumed the vertical reaction force was applied at the centre of the circular area of the assumed rigid plywood mat, and the resulting stress dissipated with depth was in the form of a trapezoid which has “2 vertical to 1 horizontal” inclined sides (Day, 2012; West, 2010). The Boussinesq developed the solution for the stresses caused by a point load to further application, such as the circular area loads (Murthy, 2003; Shroff, 2003; Venkatramaiah, 2006). For our tests, this method assumed the vertical reaction force was uniformly distributed over the entire surface area of the plywood mat. The vertical stress at a depth  $z$  below the ground surface was calculated using the 2:1 Approximation (Eq. [1]) and Boussinesq Equation (Eq. [2]) given below.

$$[1] \sigma_z = \frac{P}{\frac{\pi(D+z)^2}{4}}$$

where  $P$  is the vertical outrigger reaction force,  $D$  is the diameter of plywood mat, and  $z$  is the vertical depth below the ground surface.

$$[2] \sigma_z = K_B \cdot q$$

where  $K_B$  is the Boussinesq influence coefficient and  $K_B = 1 - \left[ \frac{1}{1 + \left(\frac{R_0}{z}\right)^2} \right]^{\frac{3}{2}}$ ,  $q$  is the intensity of the vertical outrigger reaction force per unit area and  $q = \frac{P}{\pi R_0^2}$ , and  $R_0$  is the radius of plywood mat.

In addition, the soil-mat interaction was simulated with a two-dimensional (2D) axisymmetric model using the finite element analysis (FEA). Only half the cross section of the supporting plywood mat (0.1143 m in depth by 0.5334 m in length) and the soil underneath (2.54 m in depth by 2.54 m in length) were modelled based on symmetry. The far end bottom and right edge of soil were restricted from both horizontal and vertical displacements. The plywood mat and soil were modelled as linear elastic. The Young's modulus and Poisson's ratio were defined as 12.4 GPa and 0.3 for the plywood mat and 33 MPa and 0.3 for the soil (Liu, 2005). Both parts were modelled using the four-node bilinear axisymmetric quadrilateral solid elements (CAX4) with a global mesh size of 0.02 mm. Two different load applications were taken into consideration. In the first model (Figure 4a), the vertical reaction force was assumed to be uniformly distributed over an area that is equivalent to the cross sectional area of crane outrigger pad ( $R_0 = 0.2667 \text{ m} = \text{half the length of plywood mat radius}$ ). Thus, the uniform pressure was applied over the half length of the simulated plywood mat in this model. The load input was calculated by dividing the force over the crane outrigger pad, which were 827 kPa, 1021 kPa and 1234 kPa corresponding to three working radii. In the second model (Figure 4b), the load was assumed and applied as a concentrated force at the centre of the plywood mat. The load input was taken from the estimated maximum reaction forces, which were 185 kN, 228 kN and 275 kN corresponding to the three working radii.

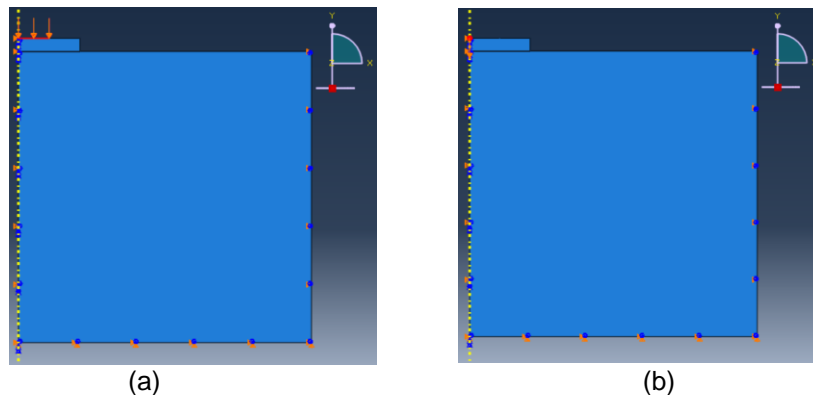
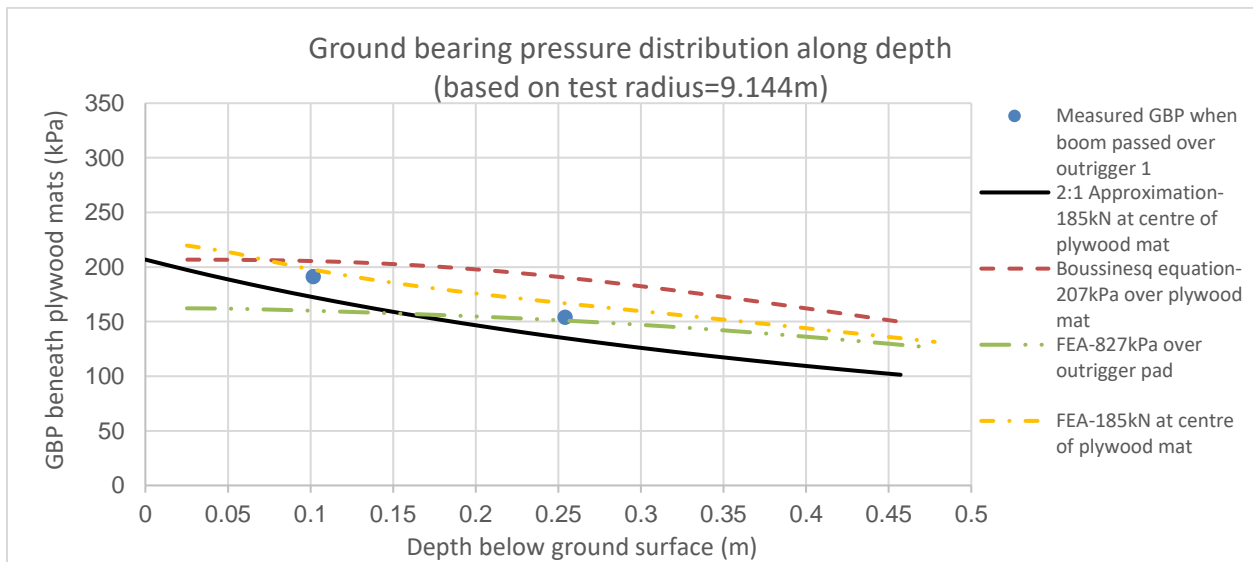


Figure 4: (a) FEA model 1 (uniformly distributed pressure) and (b) FEA model 2 (concentrated force)

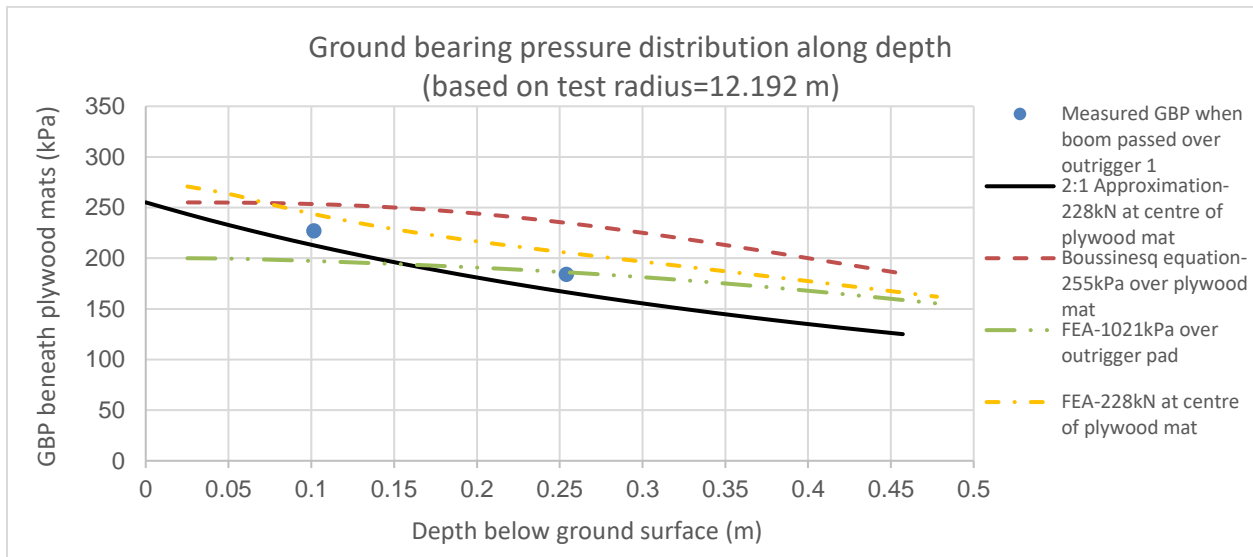
A comparison of the GBP predicted using the analytical equations and the FEA below the ground surface is shown in Figure 5 and Table 3. It is observed that the GBP decreases as the depth below the ground surface increases. The curves obtained from Boussinesq equations and FEA under the uniform pressure (model 1) have a similar trend, while the curves obtained from 2:1 approximation and FEA under the concentrated force (model 2) have a similar trend. This demonstrates that the vertical stress distribution along the depth are affected by the assumptions of the loading distribution over the ground surface. The values of GBP measured from tests are roughly between those obtained from FEA with different loading assumptions. This indicates that the force transferred from the outrigger support to the ground underneath cannot be simply assumed as a concentrated force. In reality, it is distributed to an area smaller than the cross sectional area of the crane outrigger pad. In general, the GBP distribution obtained from various methods were close to each other, and close to the actual test results. This verifies that the currently used 2:1 approximation method in predicting the GBP beneath outrigger supports is reliable but is suggested to increase the pressure by 10%. In addition, the results validate the numerical model ability to simulate the mat-soil interactions.

Table 3: Comparisons of GBP obtained from various methods at two depths below ground surface

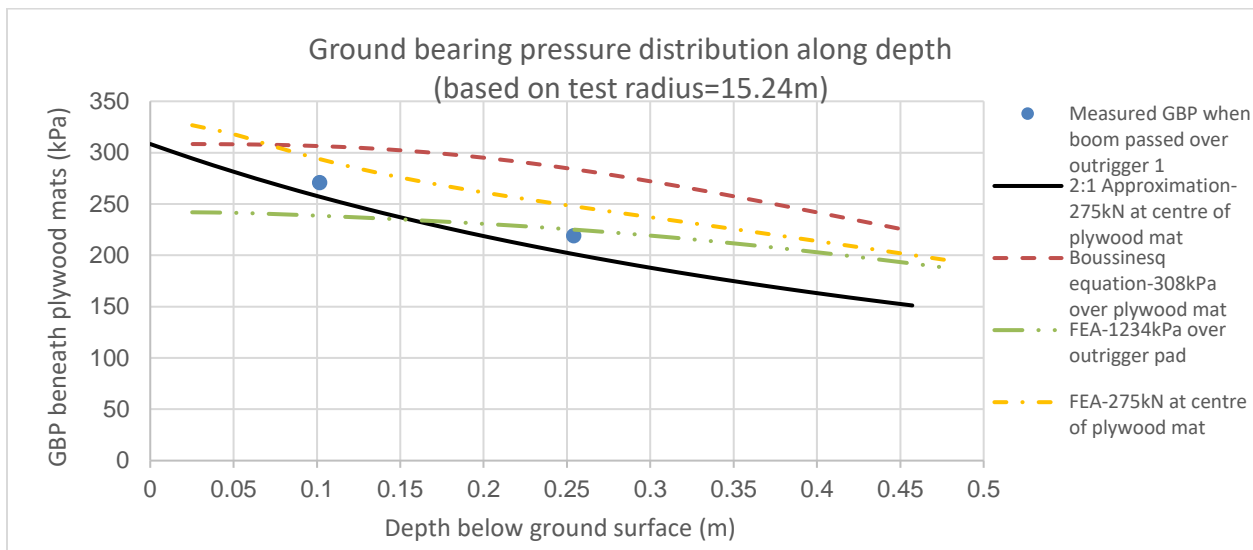
Depth below Ground Surface (m)	GBP results at $\alpha = 135^\circ$ and test radius = 9.144 m								
	Test (kPa)	2:1 Approximation		Boussinesq Eq.		FEA			
		Under concentrated force (kPa)	Difference to test results	Under uniform pressure (kPa)	Difference to test results	Under uniform pressure (kPa)	Difference to test results	Under concentrated force (kPa)	Difference to test results
0.1016	191	172	-9.9%	205	7.3%	160	-16.2%	198	3.7%
0.254	154	135	-12.3%	190	23.4%	151	-1.9%	167	8.4%
	GBP results at $\alpha = 135^\circ$ and test radius = 12.192 m								
0.1016	227	213	-6.2%	253	11.5%	197	-13.2%	244	7.5%
0.254	184	166	-9.8%	235	27.7%	186	1.1%	206	12.0%
	GBP results at $\alpha = 135^\circ$ and test radius = 15.24 m								
0.1016	271	257	-5.2%	306	12.9%	239	-11.8%	294	8.5%
0.254	219	201	-8.2%	284	29.7%	225	2.7%	248	13.2%



(a)



(b)



(c)

Figure 5: Comparison of GBP distribution ( $\alpha = 135^\circ$ ) along the depth obtained from various methods corresponding to (a) test radii of 9.144 m, (b) test radius of 12.192 m, and (c) test radius of 15.24 m

## 2.4 Data analysis and recommendations

Ground conditions routinely need to be upgraded to handle the applied loads from crane outriggers. This may involve adding a compacted gravel layer with a higher capacity than the existing ground conditions. The two layers of collected data at 4" (0.1016 m) and 10" (0.254 m) beneath the outrigger mats show consistent pressure dissipation of 19.2% over the 6" (0.1524 m) depth difference. For ease of industry use, the 2:1 approximation method can be used but increase the pressure by 10%.

## 3 Conclusions

This paper summarized the actual measurements of ground bearing pressure beneath the outrigger supports of a rough terrain crane at the PCL East module yard located in Edmonton, Alberta. Three lifting operations were performed in the investigation of outrigger support reaction, and produced nine sets of data corresponding to three critical boom positions with three working radii. The measured pressure was

collected from two pressure cells buried vertically in the ground at two different depths, which illustrated the distribution of ground bearing pressure along the depth underneath the supporting outrigger mats. The numerical mat-soil interaction models involving two scenarios were validated from the actual measurements, the 2:1 approximation method and the Boussinesq equations. The actual pressure data validated the manufacturer's outrigger loads. The currently used methods of treating the outrigger mat as a rigid body and applying the 2:1 approximation method in predicting the ground bearing pressure beneath outrigger supports is reliable but should be increased by 10%. Further work will focus on measuring and analyzing and the ground pressures underneath crawler cranes and investigating the effects of the mat and soil stiffnesses on the ground bearing pressure.

## Acknowledgements

The following financial support agencies are thankfully acknowledged: NSERC Engage Grants and PCL Industrial Management Inc.

## References

- ASME B 30.5, 2014. Mobile and locomotive cranes. The American Society of Mechanical Engineers, New York, NY, USA.
- CIRIA. 1996. Crane stability on site. CIRIA special publication 131, Construction Industry Research and Information Association, London, UK.
- CSA Z150, 2011. Safety code on mobile cranes. Canadian Standards Association, Mississauga, ON, Canada
- Day, R. W. 2012. Geotechnical engineer's portable handbook (2nd ed.). McGraw-Hill.
- Duncan, J.M., and Buchignani, A.L. 1987. Engineering Manual for Settlement Studies. Virginia Tech, Blacksburg, VA.
- Gupta, R.C. 2002. Estimating bearing capacity factors and cone tip resistance. *Soils and Foundations*, 42: 117–128. ISO. 1991. Mobile cranes – determination of stability. ISO4305:1991(E), International Organization for Standardization, Geneva, Switzerland.
- Lee, J., and Salgado, R. 2002. The estimation of the settlement of footings in sand. *International Journal of Geomechanics*, 1(2): 175-192.
- Lee, J., and Salgado, R. 2005. Estimation of bearing capacity of circular footings on sands based on cone penetration test. *Journal of Geotechnical and Geoenvironmental Engineering*, 131:442–452. doi:10.1061/(ASCE)1090-0241(2005)131:4(442).
- Liu, X. 2005. Soil bearing capacity for crawler cranes. M.Sc. thesis, Department of Civil and Environmental Engineering, University of Alberta, Edmonton, Alta.
- Liu, X., Chan, D. H., Gerbrandt, B. 2008. Bearing capacity of soils for crawler cranes. *Canadian Geotechnical Journal*, 45: 1280-1302, doi:10.1139/T08-056.
- Meyerhof, G.G. 1956. Penetration tests and bearing capacity of cohesionless soils. *Journal of the Soil Mechanics and Foundations Division*, 82(SM1): 1–19.
- Murthy, V. N. S. 2003. *Geotechnical engineering: Principles and practices of soil mechanics and foundation engineering*. Marcel Dekker, Inc., New York, NY, USA.
- Salgado, R. 2008. *The Engineering of Foundations*. McGraw-Hill, NY.
- Shapiro, H.I., Shapiro, J.P., and Shapiro, L.K. 1999. *Cranes and derricks*. 3rd ed. McGraw-Hill, New York.
- Shapiro, L. K., & Shapiro, J. P. 2011. *Cranes and derricks* (4th ed.). McGraw-Hill, New York, NY, USA.
- Shroff, A. V., & Shah, D. L. 2003. *Soil mechanics and geotechnical engineering*. A. A. Balkema Publishers, Tokyo, Japan.



Terzaghi, K. 1943. Theoretical soil mechanics. John Wiley & Sons, New York.

West, T. R. 2010. Geology applied to engineering. Waveland Press, Long Grove, IL, USA.

Venkatramaiah, C. 2006. Geotechnical engineering (Revised 3rd ed.). New Age International (P) Ltd., Daryagani, New Delhi, India.

Vesic, A.S. 1973. Analysis of ultimate loads of shallow foundations. Journal of the Soil Mechanics and Foundations Division, 99(SM1): 45–73. Liu, X., Chan, D. H., Gerbrandt, B. 2008. Bearing capacity of soils for crawler cranes. Canadian Geotechnical Journal, 45: 1280-1302, doi:10.1139/T08-056.

Tadano's Outrigger Reaction Force Supply Service. Retrieved from <https://www.tadano.co.jp/service/data/tdnsys/jackale/register.asp>

Liebherr's LICCON computer system. Retrieved from <https://www.liebherr.com/en/sau/products/mobile-and-crawler-cranes/mobile-cranes/mobile-crane-technology/crane-controller/crane-controller.html>